International Journal of Bridge Engineering (IJBE), Vol. 4, No. 1, (2016), pp. 27-55

# POST-TENSIONED BOX GIRDER BRIDGE
## An Analysis Approach using Equivalent Loads

J. Kent Hsiao[1] and Alexander Y. Jiang[2]

[1,2] Southern Illinois University Carbondale, Dept. of Civil and Environmental Engineering, USA
e-mail: hsiao@engr.siu.edu, alexjiang@siu.edu

**ABSTRACT:** Continuous-span, cast-in-place box girders have been popular in modern bridge construction. Secondary moments due to prestressing in continuous-span, post-tensioned girders, however, have significantly complicated the structural analysis and design of the girders. The equivalent load method is a commonly used method in the analysis of continuous-span, post-tensioned concrete girders since the method reduces the analysis of a prestressed structure to that of a nonprestressed structure in which the consideration of secondary moments is not required. The basic concept of the equivalent load method is that the effects of prestressing are replaced by equivalent loads produced by the prestressed tendon along the span of the structure. The approximate equivalent load method significantly simplifies the procedure for the computation of equivalent loads for post-tensioned concrete girders with parabolic tendons and therefore has commonly been used by structural engineers. In this paper, three examples of simply-supported, post-tensioned concrete girders with various combinations of locations of the centroid of tendons (c.g.s.) and the centroid of concrete (c.g.c.) are demonstrated to verify the accuracy of the approximate equivalent load method. Finally, an example of the analysis of a bridge composed of a continuous-span, post-tensioned concrete box girder superstructure and a concrete pier is also demonstrated using the approximate equivalent load method. Inconstant cross sections (inconstant c.g.c, lines) near the pier of the bridge are considered in this example.

**KEYWORDS:** Box girders; Bridge design; Continuous beams; Piers; Post tensioning.

## 1 INTRODUCTION

Continuous-span, cast-in-place, post-tensioned box girders have been popular in modern bridge construction not only because of their aesthetic appearance, but also because they provide the following advantages: (1) Post-tensioned box girder bridges allow longer spans to be constructed, which in turn allow the number of columns to be economically reduced; (2) the pier bearing assemblies

can be eliminated in continuous-span, cast-in-place box girders by utilizing monolithic connections between the bridge superstructures and the piers, which in turn eliminate the bearing assemblies maintenance problems; and (3) the post-tensioning forces enhance the control of cracking in the concrete girders [1]. Unlike simple-span, simple-supported, post-tensioned girders that can be structurally analyzed using exact methods that are not very time consuming, the secondary moments due to prestressing in continuous-span, post-tensioned girders have significantly complicated the structural analysis and design of the girders. The equivalent load method, therefore, was developed in order to simplify the analysis procedure for continuous-span, post-tensioned girders.

## 2 EXACT METHOD FOR THE COMPUTATION OF AXIAL FORCE, SHEAR, AND MOMENT

Referring to *Fig. 1*, the parabolic tendon profile along the girder is defined by

$$y = 4h\left(\frac{x^2}{L^2} - \frac{x}{L}\right) \tag{1}$$

where: h is the sag at the mid-span of the parabolic tendon,
L is the span length of the parabolic tendon.

From Eq. (1), Eq. (2) is developed:

$$y' = 4h\left(\frac{2x}{L^2} - \frac{1}{L}\right) \tag{2}$$

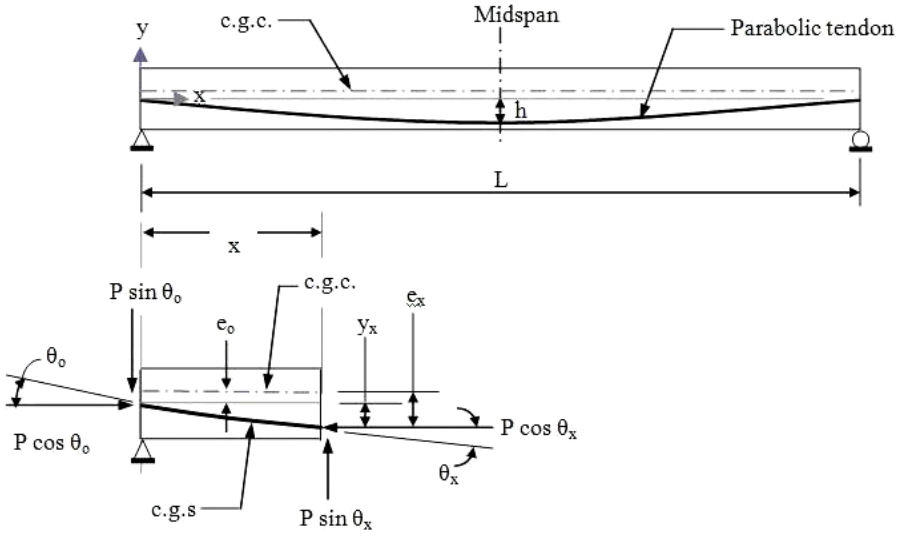


*Figure 1.* Exact method

The angle of the slope of the parabolic tendon at section x (the section at a distance of x from the left end) can be computed using Eq. (3):

$$\theta_x = \tan^{-1}|y'| \tag{3}$$

The axial force, shear, and moment at section x, therefore, are $P\cdot\cos\theta_x$, $P\cdot\sin\theta_x$, and $P\cdot\cos\theta_x\cdot(e_x)$, respectively. Note that P is the prestressing force, and $e_x$ is the vertical distance between the c.g.c line and c.g.s. line at section x. Similarly, The axial force, shear, and moment at the left end (at x = 0 m) of the girder, therefore, are $P\cdot\cos\theta_o$, $P\cdot\sin\theta_o$, and $P\cdot\cos\theta_o\cdot(e_o)$, respectively, where $\theta_o$ is angle of the slope of the parabolic tendon at x = 0 m and $e_o$ is the vertical distance between the c.g.c line and the c.g.s. line at x = 0 m.

## 3 EQUILALENT LOAD METHOD

As shown in *Fig. 2*, the basic concept of the equivalent load method is that the effects of prestressing are replaced by equivalent loads produced by the prestressing parabolic tendon along the span of the girder.

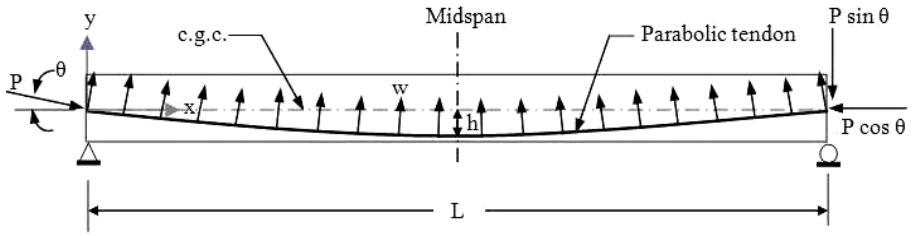


*Figure 2.* Exact equivalent load

From Eqs. (1) and (2), Eq. (4) is developed:

$$y'' = 4h\left(\frac{2}{L^2}\right) \tag{4}$$

Moreover, from Eq. (2), one has

$$\text{At } x = 0,\ y' = -4h\left(\frac{1}{L}\right)$$

$$\text{At } x = \frac{L}{2},\ y' = 0$$

$$\text{At } x = L,\ y' = 4h\left(\frac{1}{L}\right)$$

Also referring to *Fig. 2*, the distributed transverse load, w, caused by the curvature of the prestressing tendon at the contact face between the tendon and the concrete [2,3] is:

$$w = \frac{|y''|}{[1+(y')^2]^{3/2}}(P) \tag{5}$$

where: P is the prestressing force.
Note that at the mid-span (at x = L/2) of the girder, Eq. (5) turns out to be Eq. (6):

$$w = \frac{8Ph}{L^2} \tag{6}$$

Also note that at the ends of the girder (at x = 0 or L), Eq. (5) turns out to be Eq. (7):

$$w = \frac{\frac{8h}{L^2}(P)}{\left[1+(\frac{4h}{L})^2\right]^{3/2}} \tag{7}$$

Therefore, at the mid-span, the w value derived from Eq. (5) equals that shown in Eq. (6). The w value at a section becomes smaller when the section is approaching the end of the girder. At the ends, the w values are the smallest, as shown in Eq. (7). However, the deviations of the w values along the span are small since the ratio of h/L is small in post-tensioned girders.

Moreover, referring to *Fig. 3*, the vertical component of the transverse load due to prestressing force P is smaller than, but is close to, the transverse load (that is, w cos $\theta_x \approx$ w) for small values of $\theta_x$.

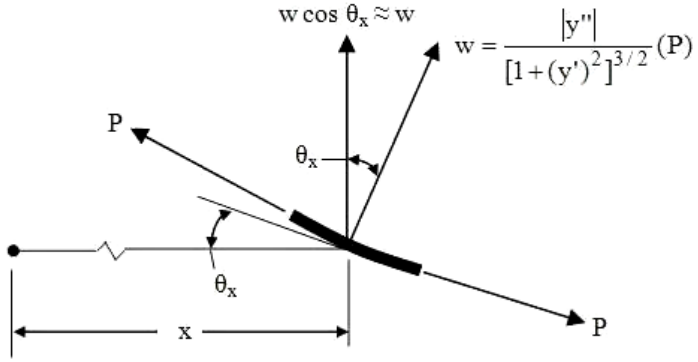


*Figure 3.* Vertical component of the transverse load due to prestressing in a parabolic tendon

Based on the above discussion, an approximate equivalent transverse load [4,5,6] as shown in *Fig. 4* has been commonly used for the analysis of post-tensioned girders. Using the approximate equivalent load to compute the axial force, shear, and moment for a post-tensioned girder is called the "approximate equivalent load method" in this paper.

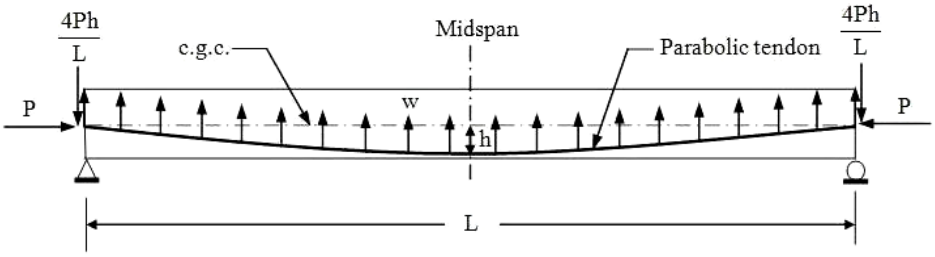


$$w = \frac{8Ph}{L^2}$$

*Figure 4.* Approximate equivalent load

## 4 ACCURACY VERIFICATION OF THE APPROXIMATE EQUIVALENT LOAD METHOD

Three examples are demonstrated for the computation of the axial force, shear, and moment along the span of post-tensioned concrete girders in order to investigate the accuracy of the approximate equivalent load method. These three examples include (1) a girder with a constant c.g.c line and a concentric c.g.s. at both ends, (2) a girder with an abrupt change of c.g.c. line and a concentric c.g.s. at both ends, and (3) a girder with an abrupt change of c.g.c. line and an eccentric c.g.s. at one end.

**Example 1:** The simply-supported, post-tensioned concrete girder shown in *Fig. 5* has a constant c.g.c. line. The parabolic c.g.s. line and the c.g.c. line are concentric at both ends of the girder (that is, the c.g.s. line is located at the same position of the c.g.c. line at both ends of the girder). The prestressing force is P = 3000 kN. Compute the axial force, shear, and moment along the span of the girder using (1) the exact method and (2) the approximate equivalent load method. Also, compare the results derived from both methods.

**Exact method:** Referring to *Figs. 1* & *5*, the angle of the slope of the c.g.s. line at the left end (at x = 0 m) of the girder can be computed using Eqs. (2) & (3):

$$\theta_o = \tan^{-1}|y'| = \tan^{-1}\left|-\frac{4(0.375\text{m})}{12\text{m}}\right| = 7.1250°$$

Therefore, the axial force and shear at the left end of the girder are $P\cdot\cos\theta_o$ = 2976.8 kN and $P\cdot\sin\theta_o$ = 372.1 kN, respectively. Also, since the c.g.s. and the c.g.c. are concentric at both ends (i.e., there is no eccentricity between the two lines at both ends), $e_o = 0$. Furthermore, since $P\cdot\cos\theta_o\cdot(e_o) = 0$, there is no moment at the left end of the girder.

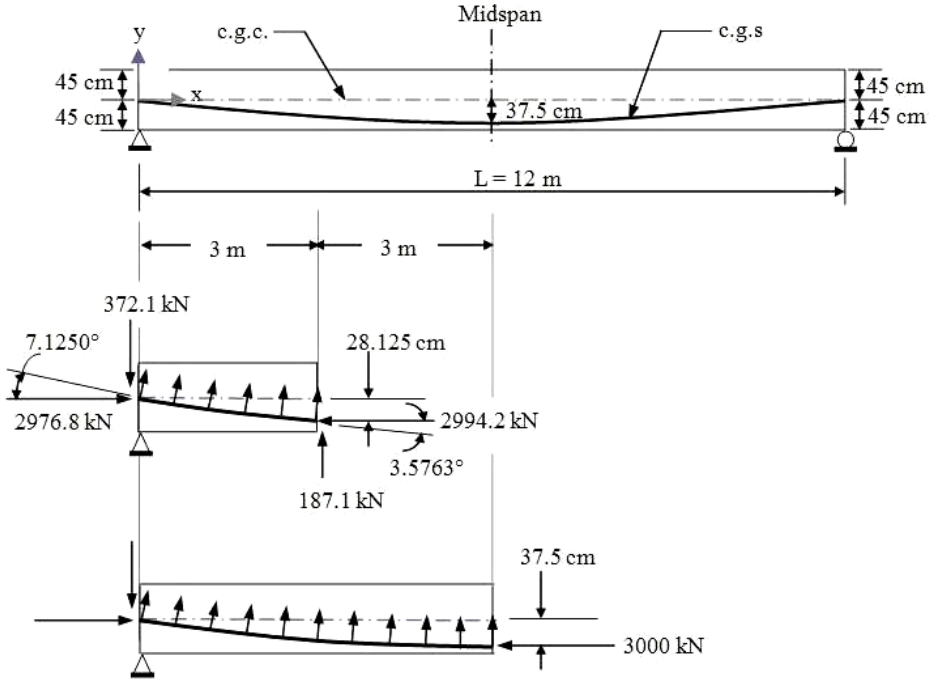


*Figure 5.* Girder with a constant c.g.c. and a concentric c.g.s. at both ends

Similarly, referring to *Figs. 1* & *5*, the angle of the slope of the c.g.s. line at a distance of x = 3 m from the left end of the girder can be computed using Eqs. (2) & (3):

$$\theta_3 = \tan^{-1}|y'| = \tan^{-1}\left|4(0.375\text{m})\left[\frac{2(3\text{m})}{(12\text{m})^2} - \frac{1}{12\text{m}}\right]\right| = 3.5763°$$

Thus, the axial force and shear of the section at x = 3 m are $P\cdot\cos\theta_3$ = 2994.2 kN and $P\cdot\sin\theta_3$ = 187.1 kN, respectively. Also, the eccentricity between the c.g.s. and c.g.c. for the section at x = 3 can be computed using Eq. (1):

$$e_3 = y = 4h\left(\frac{x^2}{L^2} - \frac{x}{L}\right) = 4(0.375\text{m})\left[\frac{(3\text{m})^2}{(12\text{m})^2} - \frac{3\text{m}}{12\text{m}}\right] = -0.28125\text{m}$$

The moment of the section at x = 3 m can thus be computed as $P\cdot\cos\theta_3\cdot(e_3)$ = 842 kN·m. Finally, using the same computation procedure, the axial force, shear, and moment at the mid-span (x = 6 m), x = 9 m, and the right end (x = 12 m) of the girder can be obtained, respectively.

**Approximate equivalent load method:** Referring to *Fig. 4*, the approximate equivalent load due to the prestressing of the parabolic tendon is uniformly

distributed along the entire length of the girder and can be computed using Eq. (6):

$$w = \frac{8Ph}{L^2} = \frac{8(3000kN)(0.375m)}{(12m)^2} = 62.5kN/m$$

The horizontal component of the prestressing force at the ends of the girder is approximately assumed to be:

$$P\cos\theta_o \approx P\cos\theta_{12} \approx P = 3000kN$$

Also, the vertical component of the prestressing force at the ends of the girder is approximately assumed to be:

$$P\sin\theta_o \approx P\sin\theta_{12} \approx w(\frac{L}{2}) = (62.5kN/m)(6m) = 375kN$$

The approximate equivalent loads acting on the girder result in the shear and moment diagrams shown in *Fig. 6*.

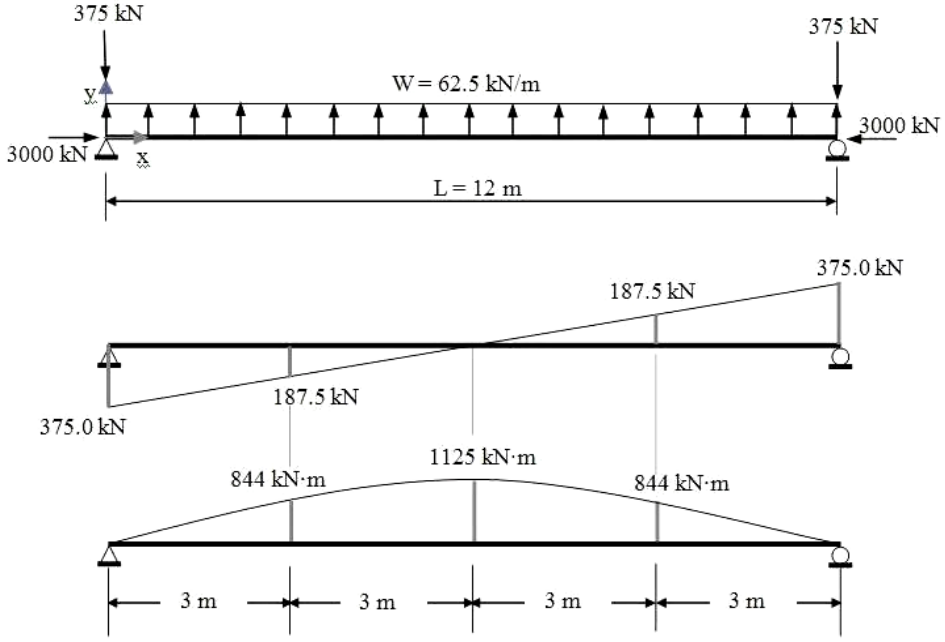


*Figure 6.* Approximate equivalent load method for Example 1

The results obtained from the exact method and the approximate equivalent load methods are summarized in Table 1. The differences between these two results are all within 1% of each other.

*Table 1.* Shear, moment, and axial force along the girder in Example 1

| force | x = 0 m | x = 3 m | x = 6 m | x = 9 m | x = 12 m |
|---|---|---|---|---|---|
| shear (exact) | 372.1 kN | 187.1 kN | 0 kN | 187.1 kN | 372.1 kN |
| shear (approximate) | 375.0 kN | 187.5 kN | 0 kN | 187.5 kN | 375.0 kN |
| moment (exact) | 0 kN·m | 842 kN·m | 1125 kN·m | 842 kN·m | 0 kN·m |
| moment (approximate) | 0 kN·m | 844 kN·m | 1125 kN·m | 844 kN·m | 0 kN·m |
| axial force (exact) | 2977 kN | 2994 kN | 3000 kN | 2994 kN | 2977 kN |
| axial force (approximate) | 3000 kN | 3000 kN | 3000 kN | 3000 kN | 3000 kN |

**Example 2:** The simply-supported, post-tensioned concrete girder shown in *Fig. 7* has an abrupt change of c.g.c. line at the mid-span. The left half of the girder is composed of a solid concrete cross-section and the parabolic tendon segment I with h = 0.375 m, as shown in *Fig. 7*, while the right half of the girder is composed of a hollow concrete cross-section and the parabolic tendon segment II with h = 0.40342 m, as shown in *Fig. 7*. The c.g.s. line is located at the same position of the c.g.c. line at both ends of the girder. The prestressing force is P = 3000 kN. Compute the axial force, shear, and moment along the span of the girder using (1) the exact method and (2) the approximate equivalent load method. Also, compare the results derived from both methods.

**Exact method:** See the procedure shown in Example 1 for the computation of the axial force, shear, and moment at the left end (x = 0 m) and at x = 3 m of the girder, respectively. Also, referring to *Figs. 1* & *7*, the angle of the slope of the c.g.s. line at the midspan (x = 6 m) of the girder can be computed using Eqs. (2) & (3):

In the parabolic tendon segment I (in which h = 0.375 m) just to the left of x = 6m,

$$\theta_6 = \tan^{-1}|y'| = \tan^{-1}\left|4(0.375\text{m})\left[\frac{2(6\text{m})}{(12\text{m})^2} - \frac{1}{12\text{m}}\right]\right| = 0°$$

In the parabolic tendon segment II (in which h = 0.40342 m) just to the right of x = 6 m,

$$\theta_6 = \tan^{-1}|y'| = \tan^{-1}\left|4(0.40342\text{m})\left[\frac{2(6\text{m})}{(12\text{m})^2} - \frac{1}{12\text{m}}\right]\right| = 0°$$

Therefore, the axial force and shear at the mid-span of the girder are $P\cdot\cos\theta_6$ = 3000 kN and $P\cdot\sin\theta_6$ = 0 kN, respectively. Also, since the eccentricity between the c.g.s. and the c.g.c. at the section just to the left of x = 6m is 0.375 m, the moment at the section can thus be computed as $P\cdot\cos\theta_6\cdot(e_6)$ = (3000 km)(0.375 m) = 1125 kN·m. Furthermore, since the eccentricity between the c.g.s. and the c.g.c. at the section just to the right of x = 6m is 0.40342 m, the moment at the section can thus be computed as $P\cdot\cos\theta_6\cdot(e_6)$ = (3000 km)(0.40342 m) = 1210 kN·m.

Similarly, referring to *Fig 7*, the angle of the slope of the c.g.s. line at a distance

of x = 9 m from the left end of the girder can be computed using Eqs. (2) & (3):

$$\theta_9 = \tan^{-1}|y'| = \tan^{-1}\left|4(0.40342\text{m})\left[\frac{2(9\text{m})}{(12\text{m})^2} - \frac{1}{12\text{m}}\right]\right| = 3.8466°$$

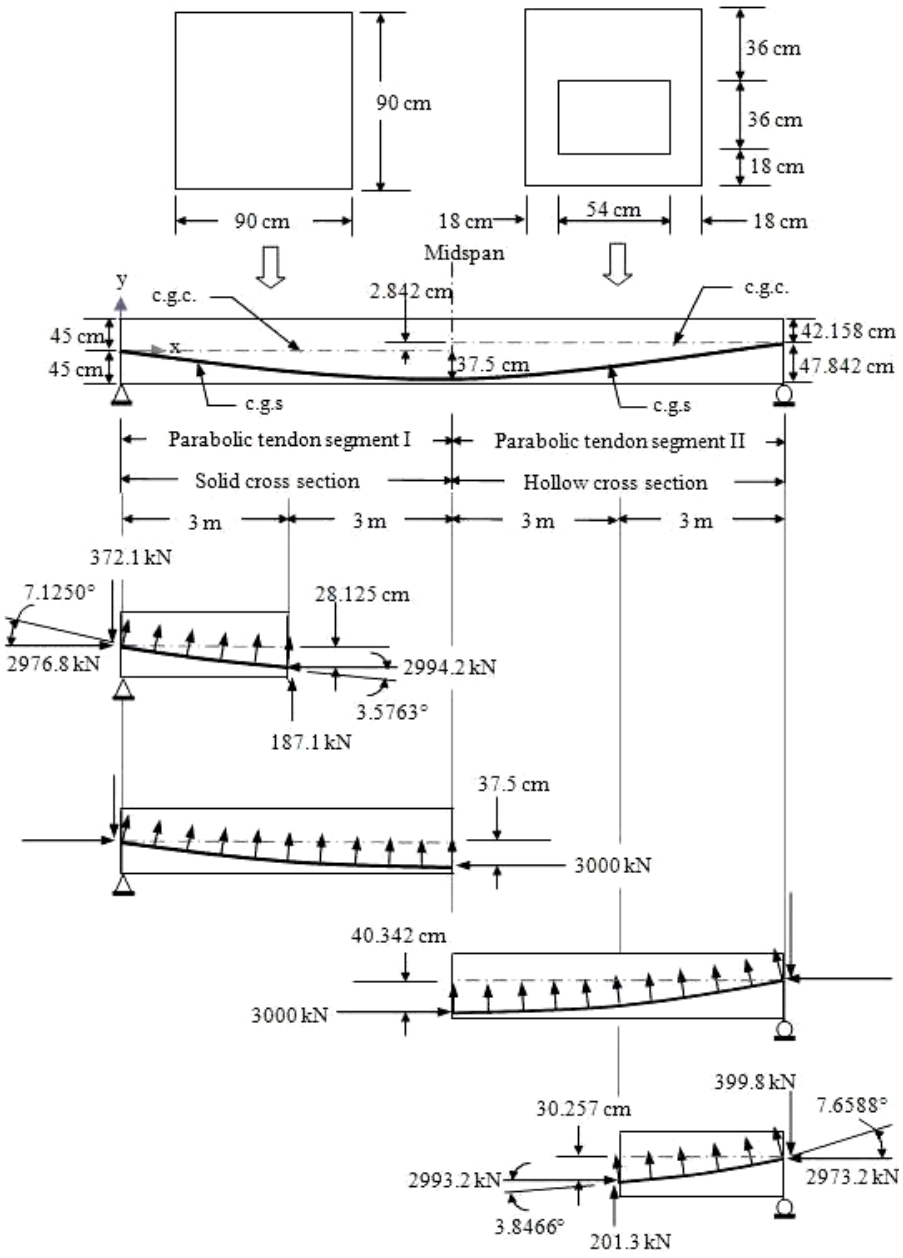


*Figure 7.* Girder with an abrupt change of c.g.c. line and a concentric c.g.s. at both ends

Thus, the axial force and shear of the section at x = 9 m are $P\cdot\cos\theta_9 = 2993.2$ kN and $P\cdot\sin\theta_9 = 201.3$ kN, respectively. Also, the eccentricity between the c.g.s. and c.g.c. for the section at x = 9 can be computed using Eq. (1):

$$e_9 = y = 4h\left(\frac{x^2}{L^2} - \frac{x}{L}\right) = 4(0.40342\text{m})\left[\frac{(9\text{m})^2}{(12\text{m})^2} - \frac{9\text{m}}{12\text{m}}\right] = -0.30257\text{m}$$

The moment of the section at x = 9 m can thus be computed as $P\cdot\cos\theta_9\cdot(e_9) = 906$ kN·m.

Finally, referring to *Fig. 7*, the angle of the slope of the c.g.s. line at the right end (x = 12 m) of the girder can be computed using Eqs. (2) & (3):

$$\theta_{12} = \tan^{-1}|y'| = \tan^{-1}\left|4(0.40342\text{m})\left[\frac{2(12\text{m})}{(12\text{m})^2} - \frac{1}{12\text{m}}\right]\right| = 7.6588°$$

Therefore, the axial force and shear at the right end of the girder are $P\cdot\cos\theta_{12} = 2973.2$ kN and $P\cdot\sin\theta_o = 399.8$ kN, respectively. Also, since the c.g.s. and the c.g.c. are concentric at both ends (i.e., there is no eccentricity between the two lines at the right end), $e_{12} = 0$. Furthermore, since $P\cdot\cos\theta_{12}\cdot(e_{12}) = 0$, there is no moment at the right end of the girder.

**Approximate equivalent load method:** Referring to *Fig. 4*, the approximate equivalent load due to the prestressing of the parabolic tendon segment I (shown in *Fig. 7*) is uniformly distributed along the left part of the girder and can be computed using Eq. (6):

$$w_I = \frac{8Ph_I}{L_I^2} = \frac{8(3000\text{kN})(0.375\text{m})}{(12\text{m})^2} = 62.5\text{kN/m}$$

Similarly, the approximate equivalent load due to the prestressing of the parabolic tendon segment II (shown in *Fig. 7*) is uniformly distributed along the right part of the girder and can be computed using Eq. (6):

$$w_{II} = \frac{8Ph_{II}}{L_{II}^2} = \frac{8(3000\text{kN})(0.40342\text{m})}{(12\text{m})^2} = 67.237\text{kN/m}$$

Also, since the angles of the slopes of the c.g.s. line at both ends (at x = 0 m and 12 m) of the girder are small, the horizontal components of the prestressing force at the ends of the girder are approximately assumed to be:

$$P\cos\theta_o \approx P\cos\theta_{12} \approx P = 3000\text{kN}$$

Furthermore, the vertical components of the prestressing force at the ends of the girder are approximately assumed to be:

$$\text{At x = 0 m, } P\sin\theta_o \approx w_I(\frac{L_I}{2}) = (62.5\text{kN/m})(6\text{m}) = 375\text{kN}$$

$$\text{At x = 12 m, } P\sin\theta_{12} \approx w_{II}(\frac{L_{II}}{2}) = (67.237\text{kN/m})(6\text{m}) = 403.4\text{kN}$$

In addition, since the elevation change of the c.g.c. at x = 6 m is 2.842 cm (shown in *Fig. 7*), the moment (the equivalent load) induced by the abrupt change of the c.g.c. line at x = 6 m can be computed as:

$$M_6 = (3000\text{kN})(0.02842\text{m}) = 85\ \text{kN·m (in the counterclockwise direction)}$$

The approximate equivalent loads acting on the girder result in the shear and moment diagrams shown in *Fig. 8*.

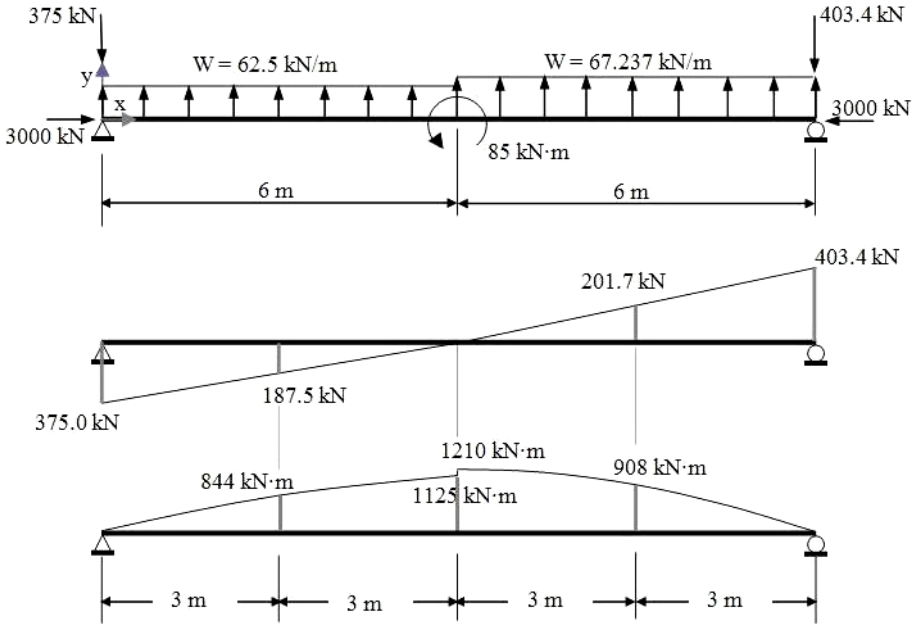


*Figure 8.* Approximate equivalent load method for Example 2

The results obtained from the exact method and the approximate equivalent load methods are summarized in Table 2. The differences between these two results are all within 1% of each other.

*Table 2.* Shear, moment, and axial force along the girder in Example 2

| force | x = 0 m | x = 3 m | just to the left of x = 6 m | just to the right of x = 6 m | x = 9 m | x = 12m |
|---|---|---|---|---|---|---|
| shear (exact) | 372.1 kN | 187.1 kN | 0 kN | 0 kN | 201.3 kN | 399.8 kN |
| shear (approximate) | 375.0 kN | 187.5 kN | 0 kN | 0 kN | 201.7 kN | 403.4 kN |
| Moment (exact) | 0 kN·m | 842 kN·m | 1125 kN·m | 1210 kN·m | 906 kN·m | 0 kN·m |
| moment (approximate) | 0 kN·m | 844 kN·m | 1125 kN·m | 1210 kN·m | 908 kN·m | 0 kN·m |
| axial force (exact) | 2977 kN | 2994 kN | 3000 kN | 3000 kN | 2993 kN | 2973 kN |
| axial force (approximate) | 3000 kN | 3000 kN | 3000 kN | 3000 kN | 3000 kN | 3000 kN |

**Example 3:** The simply-supported, post-tensioned concrete girder shown in *Fig. 9* has an abrupt change of c.g.c. line at x = 3 m from the left end of the girder. The portion of the girder from the left end to the section at x = 3 m is composed of the solid concrete cross-section, as shown in *Fig. 8*, while the portion from the section at x = 3 m to the right end of the girder is composed of the hollow concrete cross-section, as shown in *Fig. 8*. The c.g.s. line is located at the same position of the c.g.c. line at the left end of the girder, while there is an eccentricity of 2.842 cm between the c.g.s. and the c.g.c. at the right end of the girder. The prestressing force is P = 3000 kN. Compute the axial force, shear, and moment along the span of the girder using (1) the exact method and (2) the approximate equivalent load method. Also, compare the results derived from both methods.

**Exact method:** See the procedure shown in Example 1 for the computation of the axial force and shear at x = 0 m, 3 m, 6 m, 9 m, and 12 m, respectively. The computed axial forces and shears are shown in *Fig. 9*. Referring to *Fig. 9*, the moment at each section can thus be computed as: (1) at the left end of the girder (x = 0 m), moment = $P \cdot \cos\theta_o \cdot (e_o)$ = (2976.8 kN)·(0) = 0; (2) at the section just to the left of x = 3 m, moment = $P \cdot \cos\theta_3 \cdot (e_3)$ = (2994.2 kN)·(0.28125 m) = 842 kN·m; (3) at the section just to the right of x = 3m, moment = (2994.2 kN)·(0.30967 m) = 927 kN·m; (4) at x = 6 m, moment = (3000 kN)·(0.40342 m) = 1210 kN·m; (5) at x = 9 m, moment = (2994.2 kN)·(0.30967 m) = 927 kN·m; and (6) at the right end of the girder (x = 12 m), moment = (2976.8 kN)·(0.02842 m) = 84.6 kN·m.

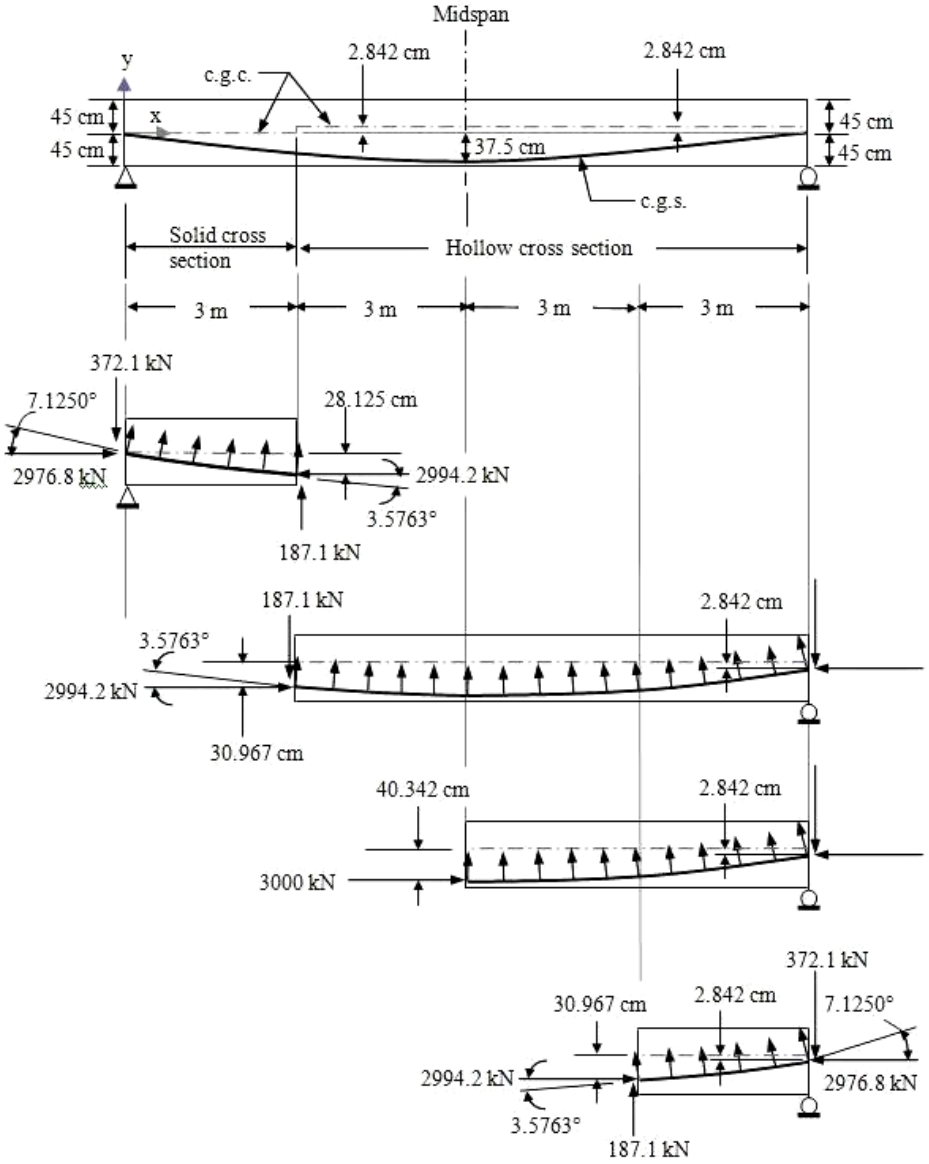


*Figure 9.* Girder with an abrupt change of c.g.c. line and an eccentric c.g.s. at one end

**Approximate equivalent load method:** See the procedure shown in Example 1 for the computation of the approximate equivalent uniformly distributed load acting along the span of the girder and the approximate equivalent vertical and horizontal loads (the approximate vertical and horizontal components of the prestressing force) acting at the ends of the girder, as shown in *Fig. 10.*

In addition, since the elevation change of the c.g.c. at x = 3 m is 2.842 cm (shown in *Fig. 9*), the moment (the equivalent load) induced by the abrupt change of the c.g.c. line at x = 3 m can be computed as:

$$M_3 = (3000\text{kN})(0.02842\text{m}) = 85\,\text{kN·m} \text{ (in the counterclockwise direction)}$$

Moreover, since there is an eccentricity of $e_{12}$ = 2.842 cm between the c.g.s. and the c.g.c. at the right end (x = 12 m) of the girder, the moment (the equivalent load) induced by the eccentricity at x = 12 m can be computed as:

$$M_{12} = (3000\text{kN})(0.02842\text{m}) = 85\,\text{kN·m} \text{ (in the clockwise direction)}$$

The approximate equivalent loads acting on the girder result in the shear and moment diagrams shown in *Fig. 10*.

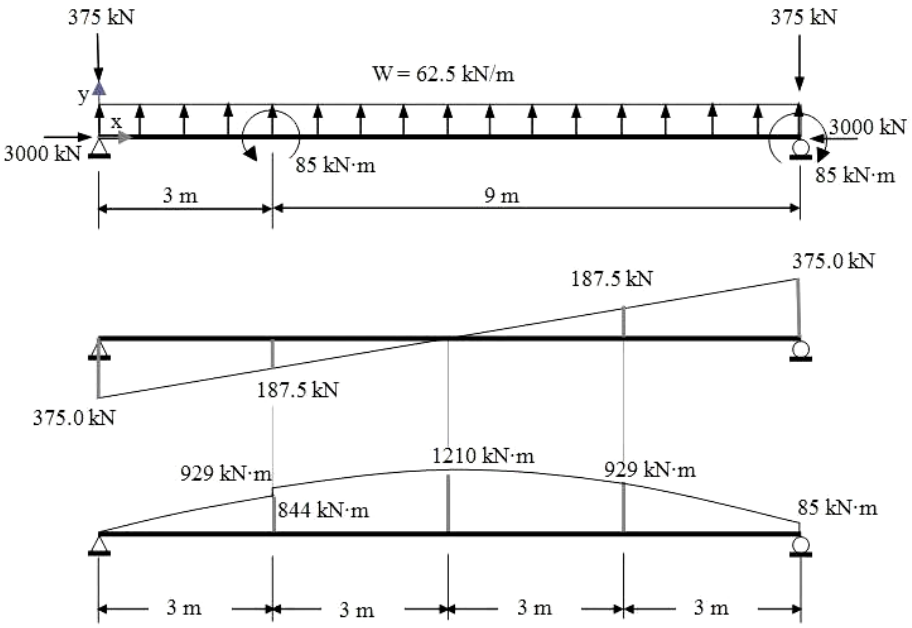


*Figure 10.* Approximate equivalent load method for Example 3

The results obtained from the exact method and the approximate equivalent load methods are summarized in Table 3. The differences between these two results are all within 1% of each other.

*Table 3.* Shear, moment, and axial force along the girder in Example 3

| force | x = 0 m | just to the left of x = 3 m | just to the right of x = 3 m | x = 6 m | x = 9 m | x = 12m |
|---|---|---|---|---|---|---|
| shear (exact) | 372.1 kN | 187.1 kN | 187.1 kN | 0 kN | 187.1 kN | 372.1 kN |
| shear (approximate) | 375.0 kN | 187.5 kN | 187.5 kN | 0 kN | 187.5 kN | 375.0 kN |
| moment (exact) | 0 kN·m | 842 kN·m | 927 kN·m | 1210 kN·m | 927 kN·m | 84.6 kN·m |
| moment (approximate) | 0 kN·m | 844 kN·m | 929 kN·m | 1210 kN·m | 929 kN·m | 85 kN·m |
| axial force (exact) | 2977 kN | 2994 kN | 2994 kN | 3000 kN | 2994 kN | 2977 kN |
| axial force (approximate) | 3000 kN | 3000 kN | 3000 kN | 3000 kN | 3000 kN | 3000 kN |

# 5 CONTINUOUS-SPAN, POST-TENSIONED BOX GIRDER BRIDGE ANALYSIS EXAMPLE USING THE APPROXIMATE EQUIVALENT LOAD METHOD

## 5.1 Bridge geometry

The following information is given for this post-tensioned box girder bridge analysis example: (1) The bridge has a continuous two-span, cast-in-place, box girder superstructure; (2) The longitudinal frame system of the bridge is shown in *Fig. 11*; (3) The span length of the two spans are 160 feet (48.768 m) and 150 feet (45.720 m), respectively; (4) The prestressing force acting along the tendon in the superstructure is 7730 kips (34,383 kN). (5) The cross section of the pier is shown in *Fig. 12*; and (6) The transverse cross section of the box girder is shown in *Fig. 13 (a)* and *(b)*.

*Fig. 13 (a)* shows that the soffit (the bottom slab of the box girder) is typically 6 inches (152 mm) thick and flared to 12 inches (305 mm) thick at the section near the pier. *Fig. 13 (b)* shows the transverse cross section of the box girder at the pier.

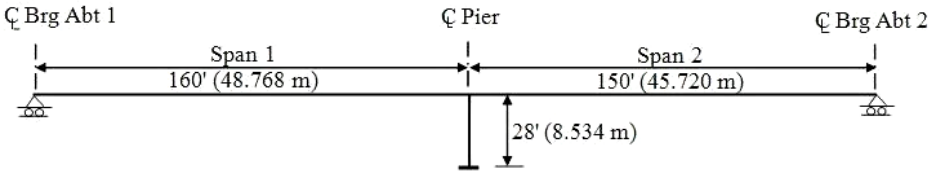


*Figure 11.* Longitudinal frame system of the bridge

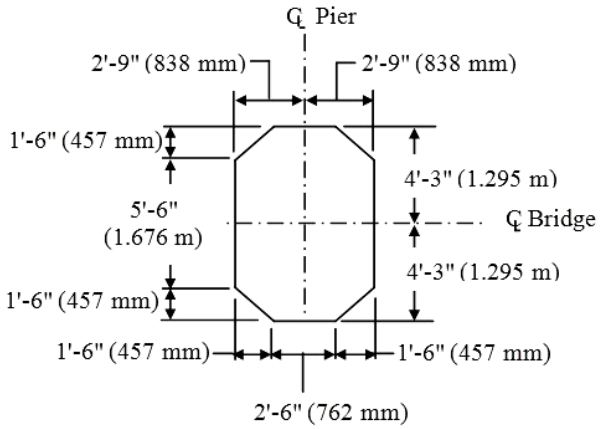


*Figure 12.* Cross section of the pier

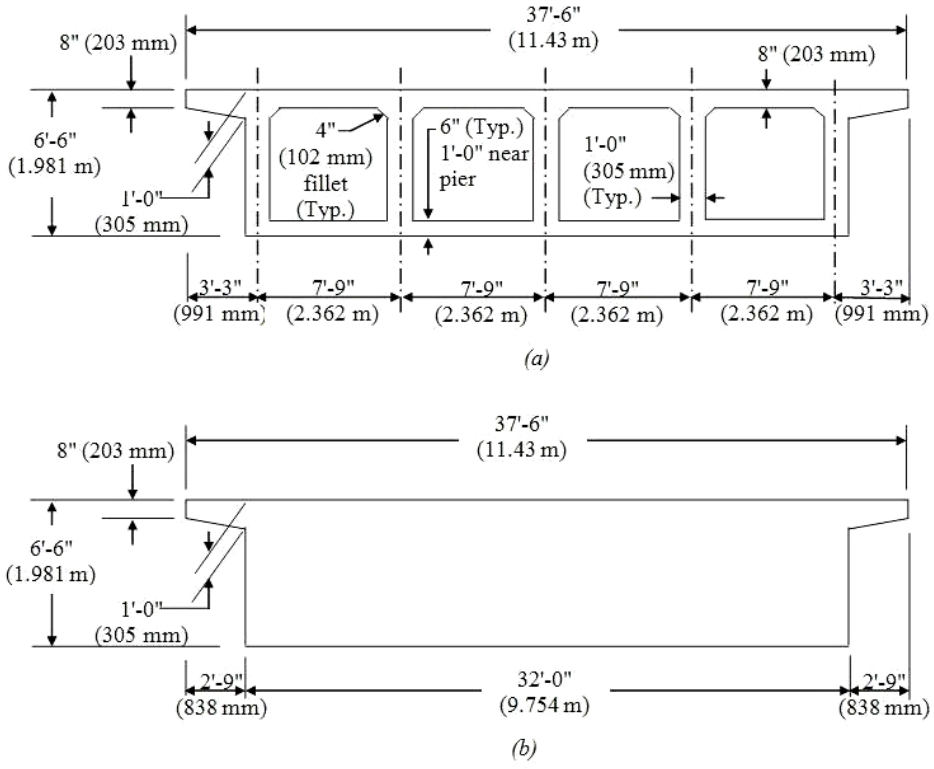


*Figure 13.* Transverse cross section of the box girder

The elevation ($y_b$) of the c.g.c. reduces as the thickness of the soffit increases as shown in Table 4. The longitudinal cross section of the box girder at the pier is

shown in *Fig 14*. Referring to *Fig. 14*, the reason for increasing the thickness of the soffit near the pier is to lower the c.g.c. of the superstructure in this area, and thus, increase the eccentricity between the c.g.s. and the c.g.c. of the superstructure near the pier. The high tensile stresses that are usually present at the top fibers of the superstructure near the pier can thus be reduced by increasing the eccentricity between the c.g.s. and the c.g.c. in this area [7].

*Table 4.* Section properties of the transverse cross sections of the box girder

| soffit | $y_t$ [a] | $y_b$ [b] | $I_g$ [c] | $A_g$ [d] |
|---|---|---|---|---|
| typical<br>6 in. (152 mm) | 2.87 ft<br>(87.5 cm) | 3.63 ft<br>(110.6 cm) | 419.8 $ft^4$<br>($362 \times 10^6$ $cm^4$) | 69.03 $ft^2$<br>(64,131 $cm^2$) |
| flared<br>8 in. (203 mm) | 3.06 ft<br>(93.3 cm) | 3.44 ft<br>(104.8 cm) | 458.8 $ft^4$<br>($396 \times 10^6$ $cm^4$) | 73.53 $ft^2$<br>(68,312 $cm^2$) |
| flared<br>10 in. (254 mm) | 3.21 ft<br>(97.8 cm) | 3.29 ft<br>(100.3 cm) | 489.6 $ft^4$<br>($423 \times 10^6$ $cm^4$) | 78.03 $ft^2$<br>(72,492 $cm^2$) |
| flared<br>12 in. (305 mm) | 3.34 ft<br>(101.8 cm) | 3.16 ft<br>(96.3 cm) | 513.5 $ft^4$<br>($443 \times 10^6$ $cm^4$) | 82.53 $ft^2$<br>(76,673 $cm^2$) |
| Solid section | 3.19 ft<br>(97.2 cm) | 3.31 ft<br>(100.9 cm) | 768.3 $ft^4$<br>($663 \times 10^6$ $cm^4$) | 212.6 $ft^2$<br>(197,512 $cm^2$) |

[a] $y_t$ = the distance from the neutral axis of a concrete gross section, neglecting steel, to the extreme top fiber of the section.
[b] $y_b$= the distance from the neutral axis of a concrete gross section, neglecting steel, to the extreme bottom fiber of the section.
[c] $I_g$= the moment of inertia of a gross concrete section about the neutral axis of the section, neglecting steel.
[d] $A_g$= the gross area of a concrete section.

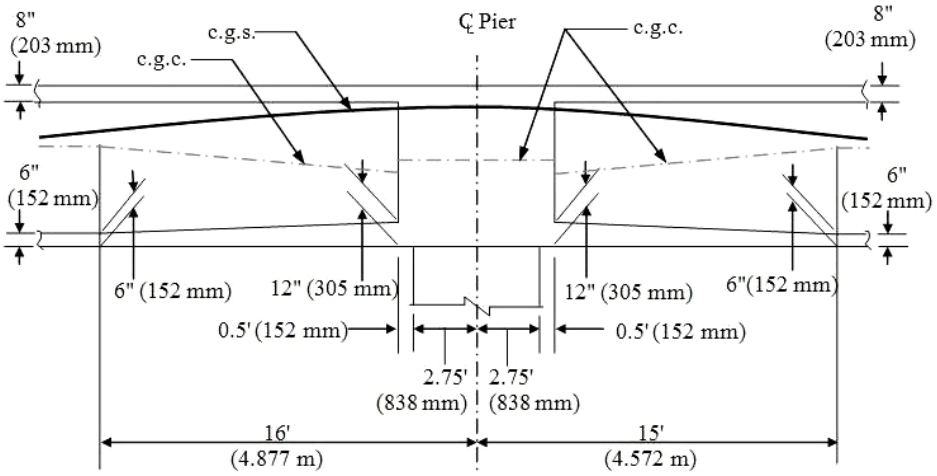


*Figure 14.* Longitudinal cross section of the box girder at the pier

## 5.2 Cable path

Placing the c.g.s. at $y_t$ = 2.87 ft (875 mm) (the location of the neutral axis of the typical cross section as shown in Table 4) in the anchor zone results in a uniform stress distribution at the ends of the girder. However, the top tendons may be too high to have sufficient top edge clearance. In order to increase edge clearance at the top, the c.g.s. is placed at the mid-height of the ends of the girder as shown in *Fig. 15*.

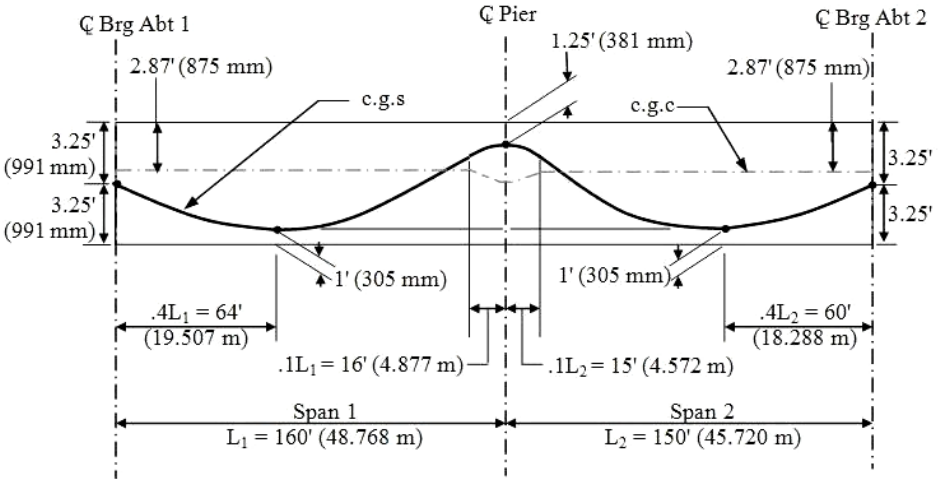


*Figure 15.* Cable path

Also, in each span, the maximum moment due to the weight of the girder is approximately located at a distance of 0.4 L from the abutment, where L is the span length. The lowest point of the c.g.s. in each span, therefore, is placed at a distance of 0.4 L from the abutment in order to balance the maximum moment at the section induced by the weight of the girder. *Fig. 15* illustrates the lowest points (at 0.4 L from the abutment) and the highest point (at the pier) of the c.g.s.

The inflection points along the cable path are located at a distance of 0.1 L from the center line of the pier. This location provides a reasonable radius of curvature for placing a semi-rigid duct [1]. Referring to *Fig. 16*, the location of the inflection point of the c.g.s. in each span can be determined using the following procedure [5]: (1) draw a line to connect the highest point of the c.g.s. in the span (at the center line of the pier) and the lowest point of the c.g.s, in the span (at 0.4 L from the abutment, i.e., at 0.6 L from the center line of the pier), (2) draw a vertical line at a distance of 0.1 L from the center line of the pier, (3) find the location of the inflection point (the intersection of these two lines).

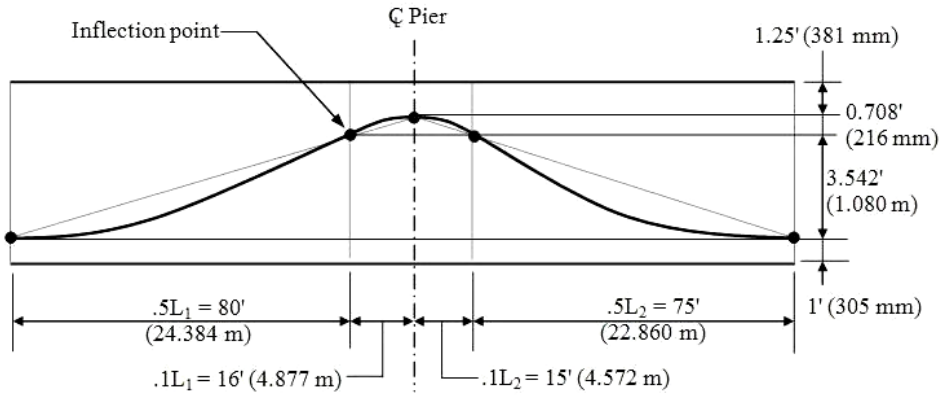


*Figure 16.* Locations of inflection points

## 5.3 Equivalent loads produced by prestressing

As shown in *Fig. 17*, the tendon profile in each span of the girder is made of three parabolas. Therefore, there are a total of six parabolas in this two-span girder.

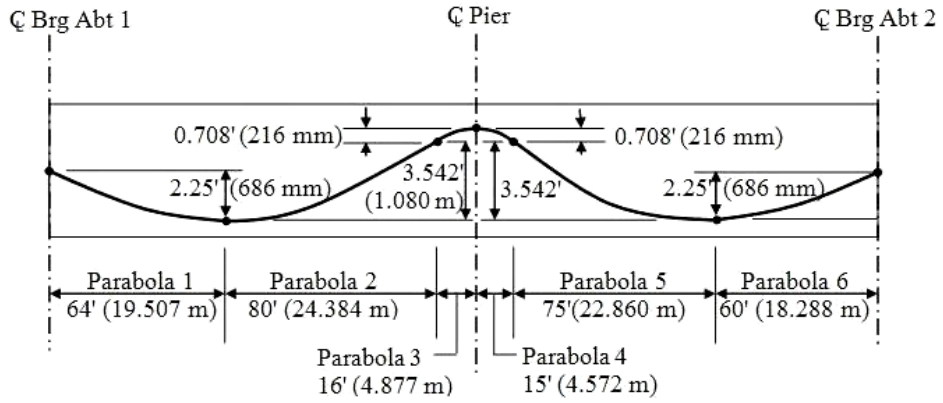


*Figure 17.* Tendon profile of the girder

Note that due to frictional and anchor set losses, the magnitude of the prestressing force acting along the tendon changes from one location to another. This example assumes that the difference between the largest and the smallest prestressing force acting along the tendon is small (say within 6% of each other), the average of these two extreme prestressing forces, therefore, is used as the constant prestressing force, 7730 kips (34,383 kN), acting along the entire length of the tendon.

Referring to *Fig. 17*, the approximate uniformly distributed equivalent load due to the prestressing of the tendon can be computed using Eq. (6) for each

parabola:

For Parabola 1: $w_1 = \frac{8Ph_1}{L_1^2} = \frac{8(7730\text{kips})(2.25\text{ft})}{(128\text{ft})^2} = 8.492\text{kip/ft}\,(123.9\text{kN/m}) \uparrow$

For Parabola 2: $w_2 = \frac{8Ph_2}{L_2^2} = \frac{8(7730\text{kips})(3.542\text{ft})}{(160\text{ft})^2} = 8.556\text{kip/ft}\,(124.9\text{kN/m}) \uparrow$

For Parabola 3: $w_3 = \frac{8Ph_3}{L_3^2} = \frac{8(7730\text{kips})(0.708\text{ft})}{(32\text{ft})^2} = 42.757\text{kip/ft}\,(623.9\text{kN/m}) \downarrow$

For Parabola 4: $w_4 = \frac{8Ph_4}{L_4^2} = \frac{8(7730\text{kips})(0.708\text{ft})}{(30\text{ft})^2} = 48.647\text{kip/ft}\,(709.9\text{kN/m}) \downarrow$

For Parabola 5: $w_5 = \frac{8Ph_5}{L_5^2} = \frac{8(7730\text{kips})(3.542\text{ft})}{(150\text{ft})^2} = 9.735\text{kip/ft}\,(142.1\text{kN/m}) \uparrow$

For Parabola 6: $w_6 = \frac{8Ph_6}{L_6^2} = \frac{8(7730\text{kips})(2.25\text{ft})}{(120\text{ft})^2} = 9.663\text{kip/ft}\,(141.0\text{kN/m}) \uparrow$

In addition, for small values of $\theta_1$ and $\theta_2$ [where $\theta_1$ and $\theta_2$ are the angles of the slopes of the parabolic tendon at the left end (at Abutment 1) and the right end (at Abutment 2), respectively], the horizontal component of the prestressing force at the ends of the girder is approximately assumed to be:

$$P\cos\theta_1 \approx P\cos\theta_2 \approx P = 7730\text{kips}(34{,}383\text{kN})$$

Also, the vertical component of the prestressing force at the left end (at Abutment 1) of the girder is approximately assumed to be:

$$P\sin\theta_1 \approx (8.492\text{kip/ft})(64\text{m}) = 543.5\text{kips}(2417\text{kN}) \downarrow$$

Similarly, the vertical component of the prestressing force at the right end (at Abutment 2) of the girder is approximately assumed to be

$$P\sin\theta_2 \approx (9.663\text{kip/ft})(60\text{m}) = 579.8\text{kips}(2579\text{kN}) \downarrow$$

Moreover, since there is an eccentricity of $e_1$ = 0.38 ft (116 mm) between the c.g.s. and the c.g.c. at the left end (at Abutment 1) of the girder, the moment (the equivalent load) induced by the eccentricity can be computed as:

$$M_1 = (7730\text{kip})(0.38\text{ft}) = 2937\ \text{kip·ft}\ (3982\ \text{kN·m})\ \text{(in the counterclockwise direction)}$$

Similarly, since there is an eccentricity of $e_2$ = 0.38 ft (116 mm) between the c.g.s. and the c.g.c. at the right end (at Abutment 2) of the girder, the moment (the equivalent load) induced by the eccentricity can be computed as:

$M_2 = (7730\text{kip})(0.38\text{ft}) = 2937\ \text{kip·ft}\ (3982\ \text{kN·m})$ (in the clockwise direction)

The approximate equivalent loads (caused by prestressing) acting on the girder, neglecting the changes of the c.g.c. near the pier, are summarized and shown in *Fig. 18*.

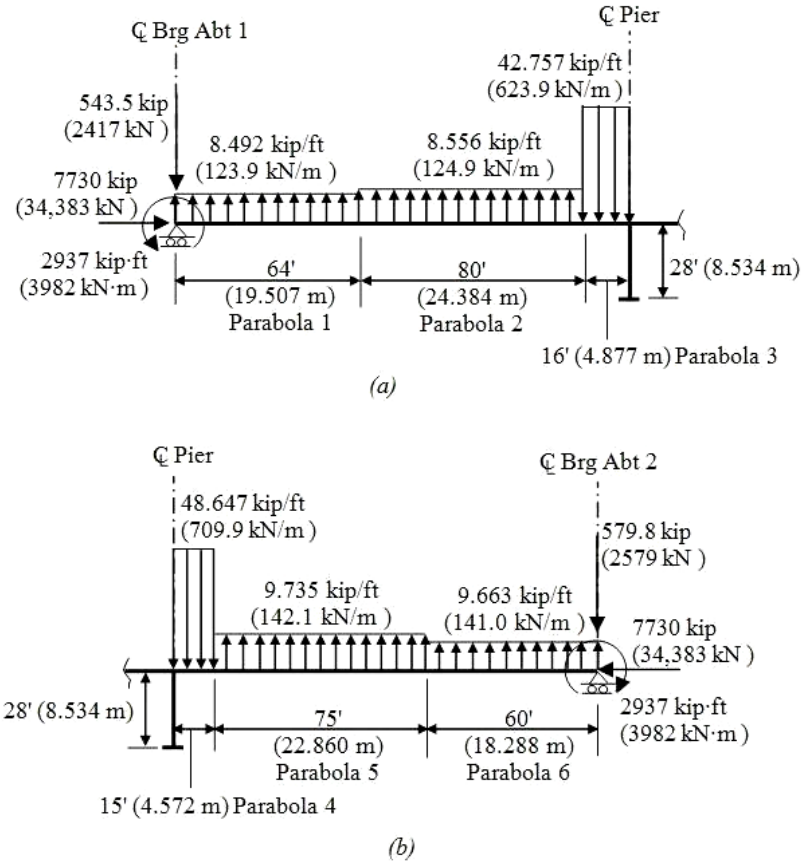


*Figure 18.* Approximate equivalent loads neglecting the changes of c.g.c. near the pier

The equivalent loads caused by the changes of the c.g.c. near the pier can be computed using the following approach:

(1) Modify the longitudinal cross section of the box girder near the pier by replacing the original flared soffit [where the soffit thickness is gradually increased from 6 inches (152 mm) to 12 inches (305 mm)] near the pier as shown in *Fig. 14* with the substitutive segmental soffits [the thicknesses of the three segments are 8 inches (203 mm), 10 inches (254 mm), and 12 inches (305 mm), respectively] as shown in *Fig. 19*.

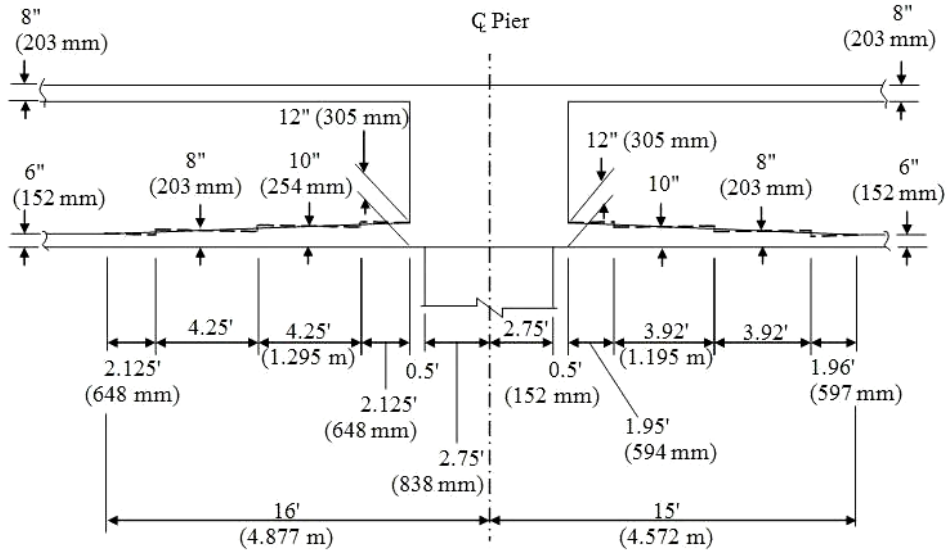


*Figure 19.* Modified longitudinal cross section of the box girder near the pier

(2) Referring to the section properties as shown in Table 4, locate the c.g.c. lines for the cross sections with the four different soffit thickness [they are 6 inches (152 mm), 8 inches (203 mm), 10 inches (254 mm), and 12 inches (305 mm), respectively] near the pier, as well as for the solid cross section at the pier. The longitudinal c.g.c. profile near and at the pier can thus be constructed and is shown in *Fig. 20*.

(3) Referring to the longitudinal c.g.c. profile near and at the pier shown in *Fig. 20*, the moments (the equivalent loads) induced by each of the abrupt changes of the c.g.c. line can be computed as the following:

At the section between the 6 in. (152 mm) soffit and the 8 in. (203 mm) soffit, the induced moment is computed as:

$$M_{6\text{–}8} = (7730\text{kip})(3.06\text{ft} - 2.87\text{ft}) = 1469\text{kip}\cdot\text{ft}\,(1992\text{kN}\cdot\text{m}).$$

At the section between the 8 in. (203 mm) soffit and the 10 in. (254 mm) soffit,

$$M_{8\text{–}10} = (7730\text{kip})(3.21\text{ft} - 3.06\text{ft}) = 1160\text{kip}\cdot\text{ft}\,(1573\text{kN}\cdot\text{m}).$$

At the section between the 10 in. (254 mm) soffit and the 12 in. (305 mm) soffit,

$$M_{10-12} = (7730\text{kip})(3.34\text{ft} - 3.21\text{ft}) = 1005\text{kip}\cdot\text{ft}\,(1363\text{kN}\cdot\text{m}).$$

At the face of the solid section,

$$M_{\text{face-of-solid}} = (7730\text{kip})(3.34\text{ft} - 3.19\text{ft}) = 1160\text{kip}\cdot\text{ft}\,(1573\text{kN}\cdot\text{m}).$$

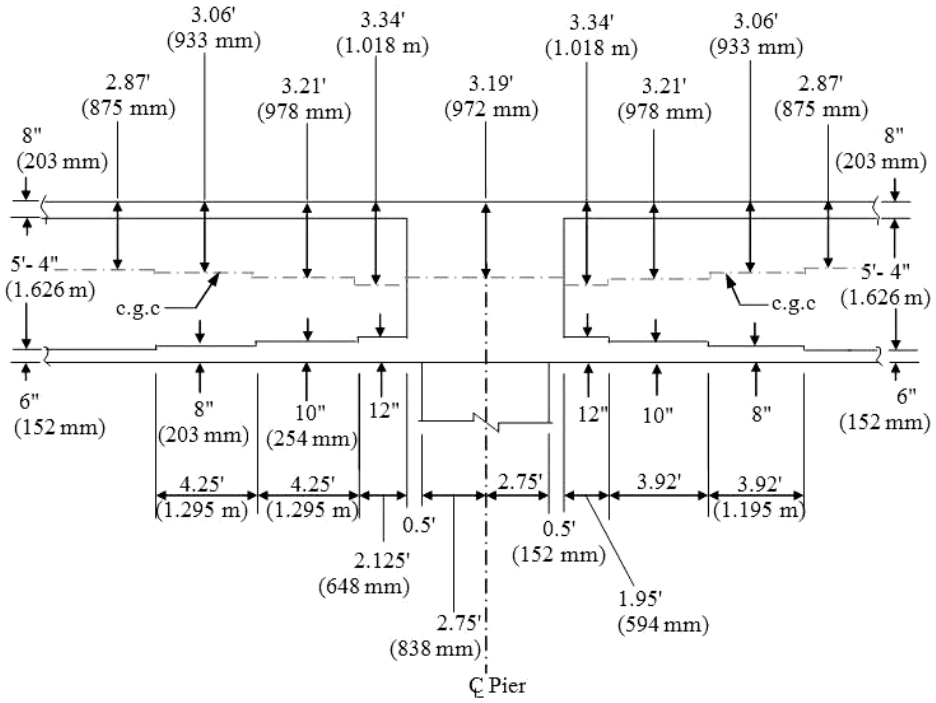


*Figure 20.* Locations of the c.g.c. lines near and at the pier

*Fig. 21* summarizes the magnitudes and the directions of the induced moments at the sections where the abrupt changes of the c.g.c. line occurred.

The combination of the equivalent loads shown in *Figs. 18* and *21* gives the total equivalent loads acting on the girder induced by the prestressing force acting on the girder.

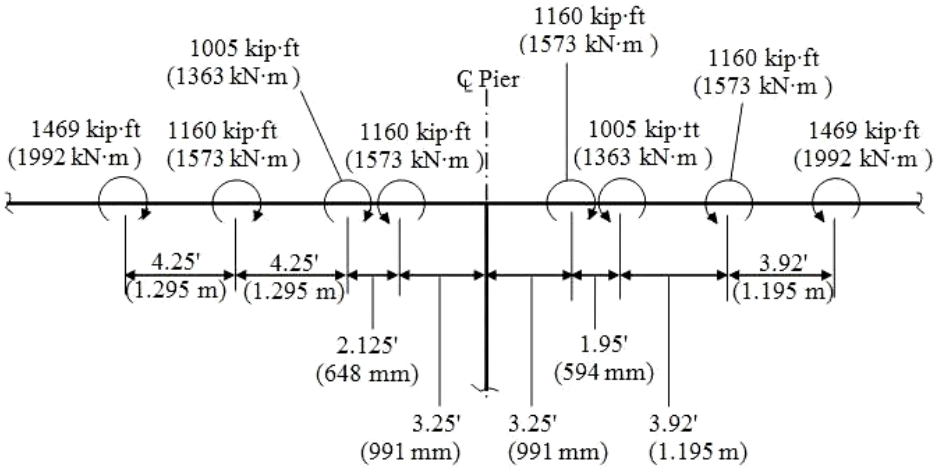


*Figure 21.* Equivalent loads induced by the abrupt changes of c.g.c. near the pier

## 5.4 Structural modeling of the post-tensioned box girder

The structural modeling of the bridge subjected to the equivalent loads can then be built as shown in *Fig. 22.*

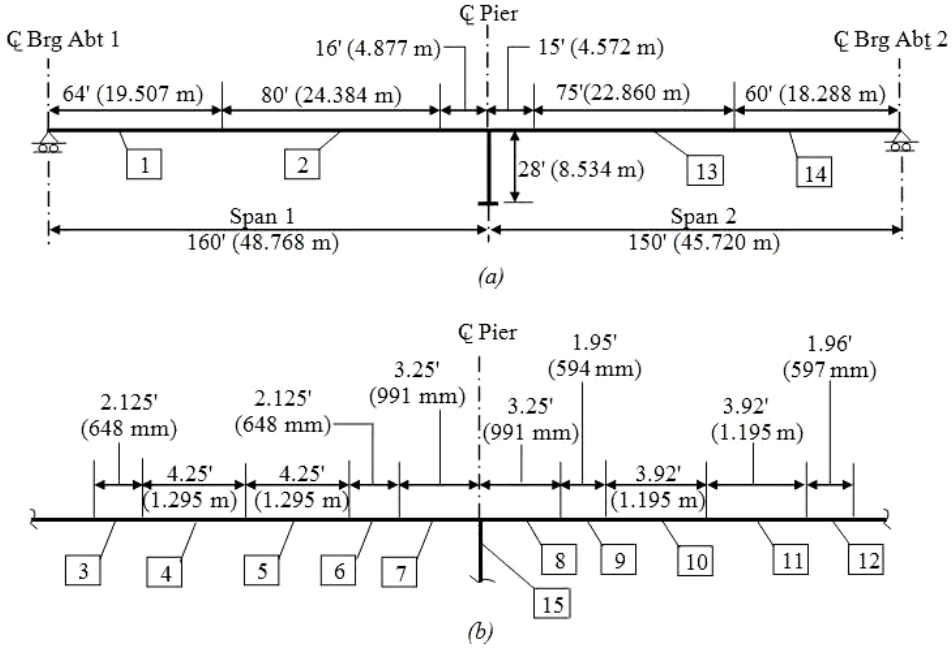


*Figure 22.* Structural modeling of the bridge

Referring to *Fig. 22*, the section properties of the structural elements are summarized in Table 5.

*Table 5*. Section properties of the structural elements

| Element(s) | Section properties |
|---|---|
| 1, 2, 3, 12, 13, and 14 | *Fig. 13(a)* typical girder section [with a 6 in. (152 mm) soffit] |
| 4 and 11 | *Fig. 13(a)* flared girder section [with a 8 in. (203 mm) soffit] |
| 5 and 10 | *Fig. 13(a)* flared girder section [with a 10 in. (254 mm) soffit] |
| 6 and 9 | *Fig. 13(a)* flared girder section [with a 12 in. (305 mm) soffit]] |
| 7 and 8 | *Fig. 13(b)* solid girder section |
| 15 | *Fig. 12* pier cross section |

## 5.5 Results of the structural analysis of the girder subjected to the equivalent loads

The elastic linear static analysis of the structural modeling (shown in *Fig. 22*) of the bridge subjected to the equivalent loads (the combination of the loads shown in *Figs. 18* and *21*) results in the moment diagram of Span 1 of the bridge shown in *Fig. 23*, and of Span 2 of the bridge shown in *Fig. 24*.

Note that the moments shown in *Figs. 23 (b)* and *24 (b)* are directly derived from the analysis of the structural model with the step-by-step-incremental [the rise of each step is 2 inches (51 mm)] soffit thickness as shown in *Fig. 20*. The final moments shown in *Figs. 23 (c)* and *24 (c)*, are then derived from *Figs. 23 (b)* and *24 (b)*, respectively, using the following procedure:

Referring to *Fig. 23(b)* and Table 5, since the section of the girder with a 7 in. (178 mm) flared soffit is located at the intersection of Element 3 [with a 6 in. (152 mm) flared soffit] and Element 4 [with a 8 in. (203 mm) flared soffit], the moment of the section with a 7 in. (178 mm) flared soffit can be computed as:

$$\frac{18{,}432\text{kip}\cdot\text{ft} + 19{,}901\text{kip}\cdot\text{ft}}{2} = 19{,}167\text{kip}\cdot\text{ft}(25{,}987\text{kN}\cdot\text{m})$$

Note that 18,432 kip·ft (24,990 kN·m) [shown in *Fig. 23(b)*] is the moment at the right end of Element 3 and 19,901 kip·ft (26,982 kN·m) [shown in *Fig. 23(b)*] is the moment at the left end of Element 4. Also note that the average of these two moments is 19,167 kip·ft (25,987 kN·m) [shown in *Fig. 23(c)*], which is the moment at the section with a 7 in. (178 mm) flared soffit of Span 1 of the bridge.

Using the same approach, the moments at the sections with a 9 in. (229 mm) and a 11" (279 mm) flared soffit, respectively, of Span 1 of the bridge can be obtained and are shown in *Fig. 23(c)*.

Similarly, using the same approach, the moments at the sections with a 7 in. (178 mm), a 9 in. (229 mm), and a 11" (279 mm) flared soffit, respectively, of Span 2 of the bridge can be obtained and are shown in *Fig. 24(c)*.

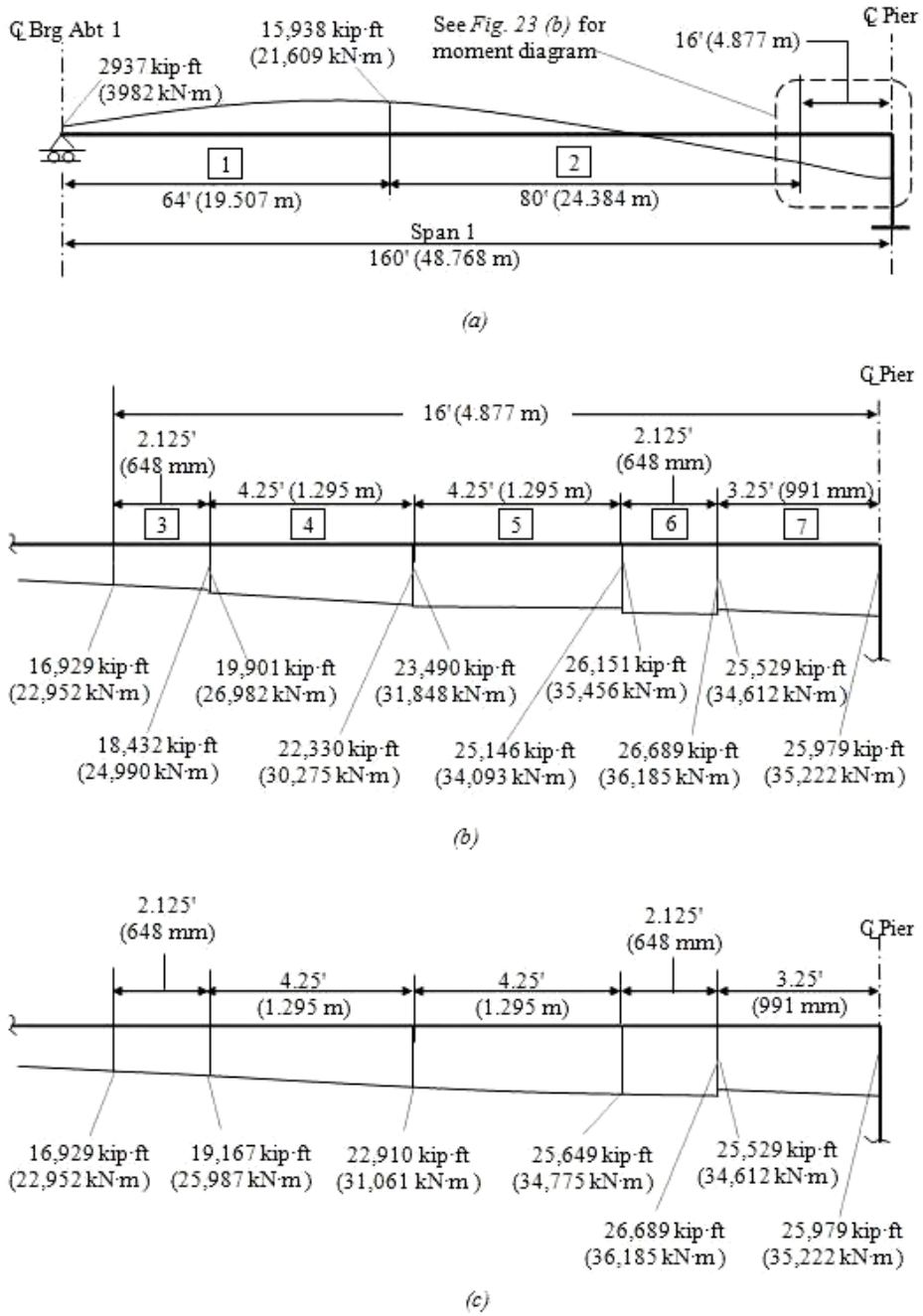


*Figure 23.* Moment diagram of Span 1 of the bridge

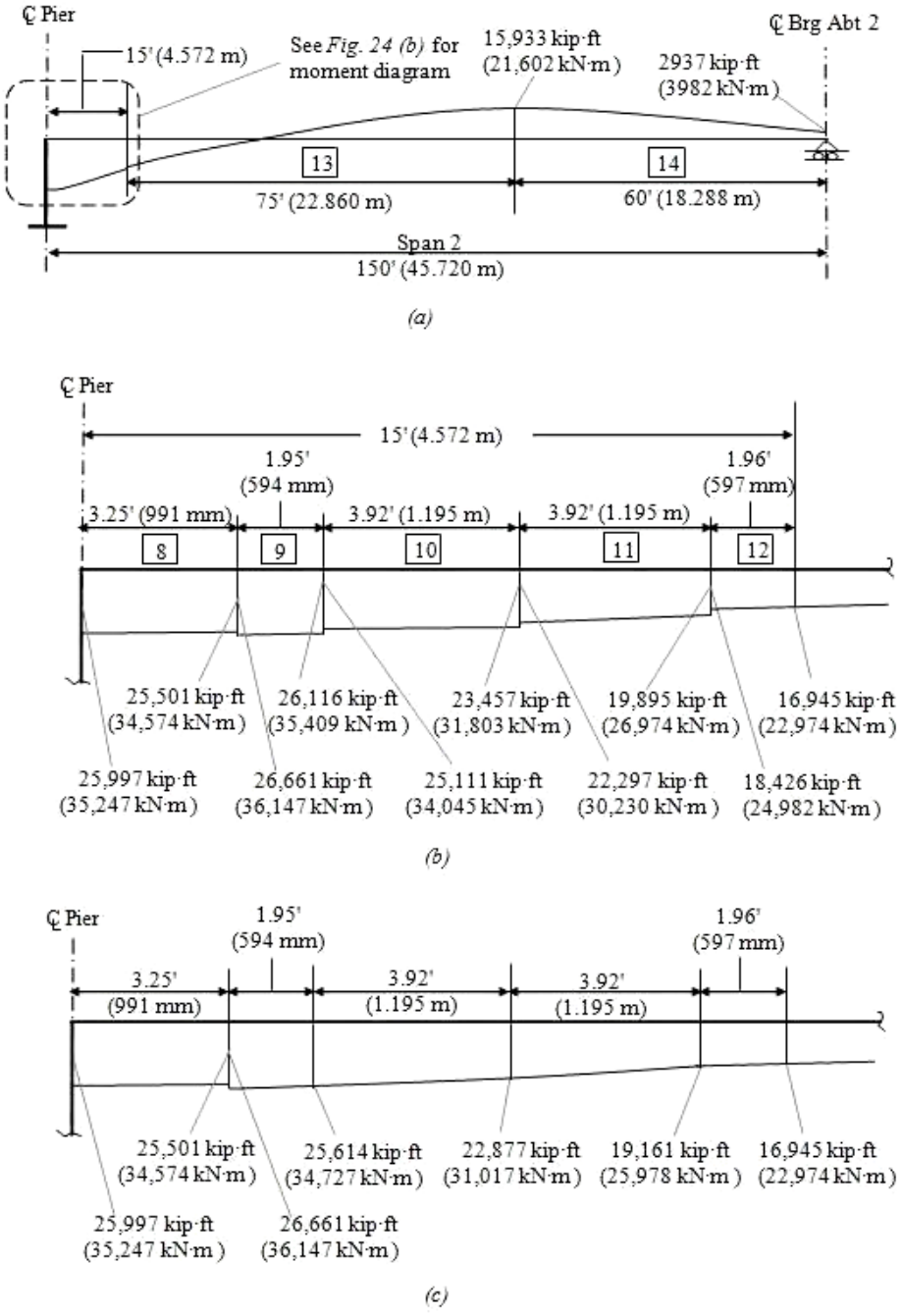


*Figure 24.* Moment diagram of Span 2 of the bridge

The moments and their corresponding locations shown in *Figs. 23 (c)* and *24 (c)* are tabulated in Tables 6 and 7, respectively.

*Table 6*. The moments and their locations within the flared-soffit range of Span 1 of the bridge

| at the section where the flared soffit begins | at the section with a 7 in. (178 mm) flared soffit | at the section with a 9 in. (229 mm) flared soffit | at the section with a 11 in. (279 mm) flared soffit | at the section where the flared soffit ends |
|---|---|---|---|---|
| 16,929 kip·ft (22,952 kN·m ) | 19,167 kip·ft (25,987 kN·m ) | 22,910 kip·ft (31,061 kN·m ) | 25,649 kip·ft (34,775 kN·m ) | 26,689 kip·ft (36,185 kN·m ) |

*Table 7*. The moments and their locations within the flared-soffit range of Span 2 of the bridge

| at the section where the flared soffit begins | at the section with a 7 in. (178 mm) flared soffit | at the section with a 9 in. (229 mm) flared soffit | at the section with a 11 in. (279 mm) flared soffit | at the section where the flared soffit ends |
|---|---|---|---|---|
| 16,945 kip·ft (22,974 kN·m ) | 19,161 kip·ft (25,978 kN·m ) | 22,877 kip·ft (31,017 kN·m ) | 25,614 kip·ft (34,727 kN·m ) | 26,661 kip·ft (36,147 kN·m ) |

## 6 CONCLUSIONS

The basic concept of the equivalent load method is that the effects of prestressing are replaced by equivalent loads produced by the prestressed tendon along the span of the structure. The equivalent load method is a commonly used method in the analysis of continuous-span, post-tensioned concrete girders since the method reduces the analysis of a prestressed structure to that of a nonprestressed structure in which the consideration of secondary moments due to prestressing is not required. The deviations of the approximate equivalent loads from the exact equivalent loads for post-tensioned concrete girders with parabolic tendons are small since the ratio of h/L (where h is the sag of the tendon and L is the length of the tendon) is small in post-tensioned girders. The approximate equivalent load method significantly simplifies the procedure for the computation of equivalent loads for post-tensioned concrete girders with parabolic tendons and therefore has commonly been used by structural engineers. In this paper, three examples of simply-supported, post-tensioned concrete girders with various combinations of locations of the centroid of tendons (c.g.s.) and the centroid of concrete (c.g.c.) are used to demonstrate the applications of the exact and the approximate equivalent load methods. The results obtained from these two methods are then compared with each other. The differences between these two results are all within 1% of each other. Finally, an example of the analysis of a continuous-span, post-tensioned

concrete box girder bridge superstructure supported by a concrete pier is also demonstrated using the approximate equivalent load method. The flared soffits of the girder near the pier of the bridge are considered in this example. This example demonstrates that the linear-incremental flared soffits near the pier can be substituted by the segmental-incremental flared soffits for the purpose of building the structural modeling of the bridge. However, due to frictional and anchor set losses, the magnitude of the prestressing force acting along the tendon changes from one location to another. Therefore, this example limits the difference between the largest and the smallest prestressing force acting along the tendon being small (say within 6% of each other) in order to use the average of these two extreme prestressing forces as the constant prestressing force acting along the entire length of the tendon.

## REFERENCES

[1] Post-Tensioning Institute, *Post-Tensioned Box Girder Bridge Manual*, Post-Tensioning Institute, 1978.

[2] Kreyszig, E, *Advanced Engineering Mathematics*, 7th Ed., John Wiley & Sons, Inc., New York, 1993.

[3] Oh, BH, Jeon, SJ, "Realistic equivalent load methods in prestressed concrete structures", KCI Concrete Journal, Vol. 13, No.1, pp. 11-17, 2001.

[4] Lin, TY, *Design of Prestressed Concrete Structures*, 2nd Ed., John Wiley & Sons, Inc., New York, 1963.

[5] Naaman, AE, *Prestressed Concrete Analysis and Design: Fundamentals*, McGraw-Hill Inc., New York, 1982.

[6] Nawy, EG, *Prestressed Concrete: A Fundamental Approach*, 5th Ed., Pearson Education, Inc., Upper Saddle River, New Jersey, 2010.

[7] California Department of Transportation, *Bridge Design Practice*, California Department of Transportation, 1993.